Z,*E* Isomerism and hindered rotations in malonamides: an NMR study of *N*,*N*′-dimethyl-*N*,*N*′-dibutyl-2-tetradecylpropane-1,3-diamide

Lydie Lefrançois,[a] Marc Hébrant,[a] Christian Tondre,[a] Jean-Jacques Delpuech,*[a] Claude Berthon[b] and Charles Madic[b]

[a] *Laboratoire de Chimie Physique Organique et Colloïdale, Unité Mixte de Recherche CNRS-UHP (UMR 7565), Université Henri Poincaré-Nancy I, B.P. 239, 54506 Nancy-Vandoeuvre Cedex, France*
[b] *CEA Valrho, DCC/DRRV/SEMP/LCTS, Marcoule, 30207 Bagnols-sur-Sèze, France*

Received (in Cambridge) 28th January 1999, Accepted 23rd March 1999

The title propane-1,3-diamide has three geometrical isomers, *ZZ*, *ZE* and *EE*, in slow exchange on the NMR timescale. The distribution of isomers involves the two amide moieties in a statistical manner. Four types of conformational changes $ZZ \rightleftharpoons ZE \rightleftharpoons EE$ are shown by exchange correlation spectroscopy and lineshape calculations. Isomers are identified on the basis of aromatic solvent induced shift (ASIS) and lanthanide induced shift (LIS) experiments. Barriers to rotation in each amide moiety are relatively low due to the bulkiness of *N*- and *C*-substituents, typically 71 kJ mol^{-1} at 25 °C, and are weakly sensitive to the conformational state (*Z* or *E*) of the other amide moiety.

Introduction

Amides have been extensively studied by nuclear magnetic resonance spectroscopy.[1] Besides classical analytical chemical uses, most of the NMR studies of this class of compounds are concerned with the partial double-bond character of the amide C(O)–N bond arising from the contribution of resonance structure **2** to the ground state of amides.[2] This electronic property

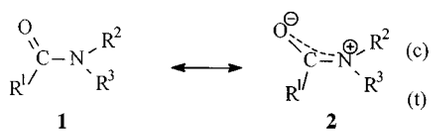

1 **2**

suggests an approximately planar amide framework and a large barrier to rotation[3,4] around the amide bond interconverting *cis* (c) and *trans* (t) substituents. In this respect, NMR investi-

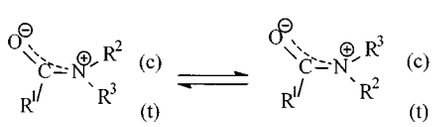

gations aim at two goals, namely (i) observing separate NMR signals for nitrogen substituents in either the *cis* or the *trans* position in symmetrically or unsymmetrically *N*-substituted amides, or, equivalently for *Z* or *E* isomers in the latter case, and (ii) measuring rotational kinetic parameters as these signals become time-averaged at higher temperatures, usually well above room temperature.

A large variety of amides have been studied from this point of view,[1] including as well as monoamides[1,5] certain classes of polyamides, such as polypeptides and proteins.[6] In the latter case, two possibilities can be envisaged concerning the number of NMR signals, namely either (i) there is no magnetic interference between the successive amide units, in which case two signals only (*Z* and *E* forms) are observed for each nucleus in each non-equivalent unit, or (ii) two neighbouring units are influencing each other, and up to four signals can be obtained in this case, corresponding to *ZZ*, *ZE*, *EZ* and *EE* forms. The latter event has rarely been mentioned in the literature. It requires the two amide moieties to be in close proximity in the magnetic interaction. This is the case when two amide moieties are directly linked to each other, as in imides[1b,7] or triacylamines[8] where a nitrogen atom is shared between two or three amide units respectively, or in hydrazine derivatives[9] where two amide moieties are linked together by an N–N bond. A few examples[7–11] are found in the literature for these cases, where the possibility of *ZZ*, *ZE*, *EZ* and *EE* forms has been considered. A less favourable situation is encountered when the two amide moieties are removed from each other by one (or, even worse, more than one) bridging carbon atom. This work reports the first successful NMR observation of *ZZ*, *ZE* and *EE* forms in the case of *N*,*N*,*N*′,*N*′-tetrasubstituted propane-1,3-diamides.

In fact, there are three ways to connect two bifunctional structural units, depending on which end of each unit is bound to the bridging carbon, namely in the present case either the carbonyl (say the "*head*") or the nitrogen atom (say the "*tail*") in each amide moiety. As in polymer science, we may thus distinguish between head to head, head to tail, and tail to tail arrangements. The head to tail arrangement is found in polypeptides. Only the *Z* isomer (in which the N–H hydrogen is *trans* to oxygen) is observed in most amino acid residues,[6] so that only *ZZ* arrangements are encountered in common polypeptides. An exception concerns *N*-substituted amino acids, *i.e.* proline,[6] or certain *N*-methylamino acids such as sarcosine,[12,13] where both forms *Z* and *E* exist in equilibrium. However no further splitting of *cis* and *trans* signals seems to have ever been mentioned in polypeptides containing such residues, *e.g.* in synthetic polyproline.[14] The tail to tail arrangement corresponds to diacylmethanediamides, a class of compounds not isolated until now, presumably due to the instability of the parent methanediamides.

Finally, head to head arrangements concern a well-known class of compounds: malonamides or propane-1,3-diamides in the IUPAC nomenclature. As in the case of polypeptides, and for the same reasons, the existence of *EZ*, *ZE* and *EE* forms besides the *ZZ* isomer is highly unlikely in the case of monosubstituted amide moieties, so that we had to envisage using *N*,*N*,*N*′,*N*′-tetrasubstituted malonamides. Our final choice *N*,*N*′-dimethyl-*N*,*N*′-dibutyl-2-tetradecylmalonamide

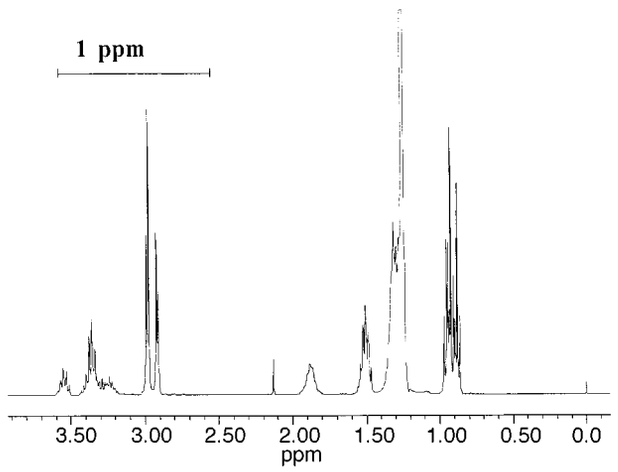

Fig. 1 ^{1}H NMR spectra of a ~0.2 molar solution of DMDBTDMA in $CDCl_3$ at 400 MHz and 25 °C.

(DMDBTDMA) was dictated by other considerations pertaining to the extracting properties of these compounds. The separation of radioelements, and especially actinides, from used nuclear fuels is an essential step in the reprocessing of spent nuclear fuel. Specific processes, like PUREX[15] or DIAMEX,[16] use for this purpose liquid–liquid extraction. To improve the efficiency of these processes, studies at the CEA,[17–19] in collaboration with European laboratories,[20] have used new extracting reagents of the diamide type, having some required properties, in the so-called DIAMEX (DIAMide EXtraction) process. DMDBTDMA proved to be one of the best suited diamides to extract trivalent actinides from nitric acid solutions into aliphatic diluents. One important problem in designing a liquid–liquid extraction system is third phase formation, *i.e.* the splitting of the organic phase into two layers when the aqueous phase is highly concentrated in solutes.[21] This is the case with DMDBTDMA, and the final goal of this NMR study is to understand third phase formation on the molecular level. From this point of view, this paper reports the very first step of these investigations with the purpose of getting information on the conformational properties of the pure reagent DMDBTDMA dissolved in a single solvent $CDCl_3$.

Experimental

Materials

N,*N*′-Dimethyl-*N*,*N*′-dibutyl-2-unsubstituted (*and* 2-tetradecyl) malonamides, DMDBMA and DMDBTDMA respectively, were obtained from Panchim (France) and were checked for purity before use. The solvents were deuterated benzene (CEA), deuterated chloroform (Euriso-top) and per-deuterated dodecane (Icon Leman). Concentrations of malonamides were in the range 0.1 to 0.2 or 0.2 to 0.5 molar for ^{1}H or ^{13}C NMR experiments, respectively. For variable-temperature kinetic measurements, the same series of capped tubes was used for all nuclei of the same type (^{1}H or ^{13}C) at all temperatures (−10 to +63 °C) in the same solvent ($CDCl_3$).

NMR Spectroscopy

^{1}H and {^{1}H} ^{13}C spectra were recorded either at 400 and 100.1 MHz on a Bruker AM-400 spectrometer with tetramethylsilane (TMS) as internal standard, or at 300 and 75.1 MHz on a Varian VRX 300 spectrometer. Variable waiting times between pulse sequences were used to obtain ^{13}C quantitative determinations of *ZZ*, *ZE* and *EE* populations. Figs. 1 and 2 present a general view of large-scale ^{1}H and ^{13}C spectra of DMDBTDMA with the objective of assigning overall frequency ranges (Table 1) to the different primary, secondary, tertiary and carbonyl carbons (and to the respective attached protons) as follows: (i) *N*-methyl, CH_3–N; terminal methyls of the *N*-butyl, CH_3(N,δ) and tetradecyl, CH_3(R) substituents; (ii) *N*-methylene, CH_2–N; terminal and central methylenes of the *N*-butyl, CH_2(N,γ) and CH_2(N,β) respectively, and *N*-tetradecyl, CH_2(R,ω) and CH_2(R) respectively, substituents; (iii) the central methine, CH; and (iv) the carbonyls CO. Lines were assigned on the following grounds: (i) use of tables of usual chemical shifts, (ii) comparison with the 2-unsubstituted analogue DMDBMA to distinguish between butyl and tetradecyl nuclei, (iii) use of the DEPT[22] sequence to distinguish between primary, secondary and tertiary carbons, and (iv) use of heteronuclear ^{13}C–^{1}H correlation spectroscopy[23,24] to assign unknown ^{13}C lines from known ^{1}H lines and *vice versa*.

Nuclear sites in mutual exchange were probed by the standard EXSY (EXchange SpectroscopY) pulse sequence D–90°–t_1–90°–t_m–90°–t_2(AQ) in phase-sensitive (TPPI) mode.[25–28] A total of 1K experiments with 8 scans of 2K data points were collected and zero-filled to obtain a 2K × 2K data matrix. Exchange rates were obtained by comparing experimental and theoretical one-dimensional lineshapes computed according to a matrix formulation (see later) from Anderson,[29] Kubo[30] and Sack,[31] with an appropriate home made program ECHGN.[32] Trial and error procedures were used to fit simultaneously two kinetic parameters k_1, k_2 by minimizing the sum of squared residues.

Table 1 ^{1}H and ^{13}C chemical shifts (ppm from TMS) of DMDBTDMA

	δ (^{13}C)	δ (^{1}H)
CH_3–N	34	2.9–3.0
CH_3(N,δ)	14	0.9
CH_3(R)	14	0.9
CH_2–N	48	3.3
CH_2(N,β)	32	1.2–1.6
CH_2(N,γ)	20	1.2–1.6
CH_2(R)	29	1.2–1.6
CH_2(R,ω)	23	1.2–1.6
CH	50	3.6
CO	170	—

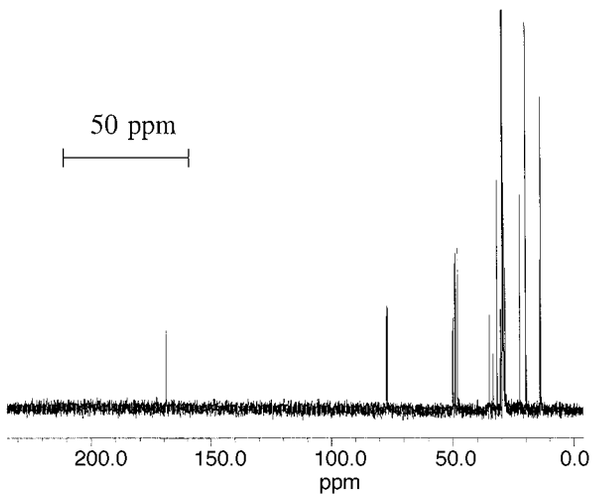

Fig. 2 ^{13}C NMR spectra of a ~0.2 molar solution of DMDBTDMA in $CDCl_3$ at 100.1 MHz and 25 °C.

Results and discussion

Line multiplicity and the existence of *Z*,*E* isomers

The four conformers expected for DMDBTDMA are shown in Scheme 1 using a conventional planar representation. Due to molecular symmetry, enantiomeric *ZE* and *EZ* isomers are indiscernible by NMR spectroscopy in optically inactive sol-

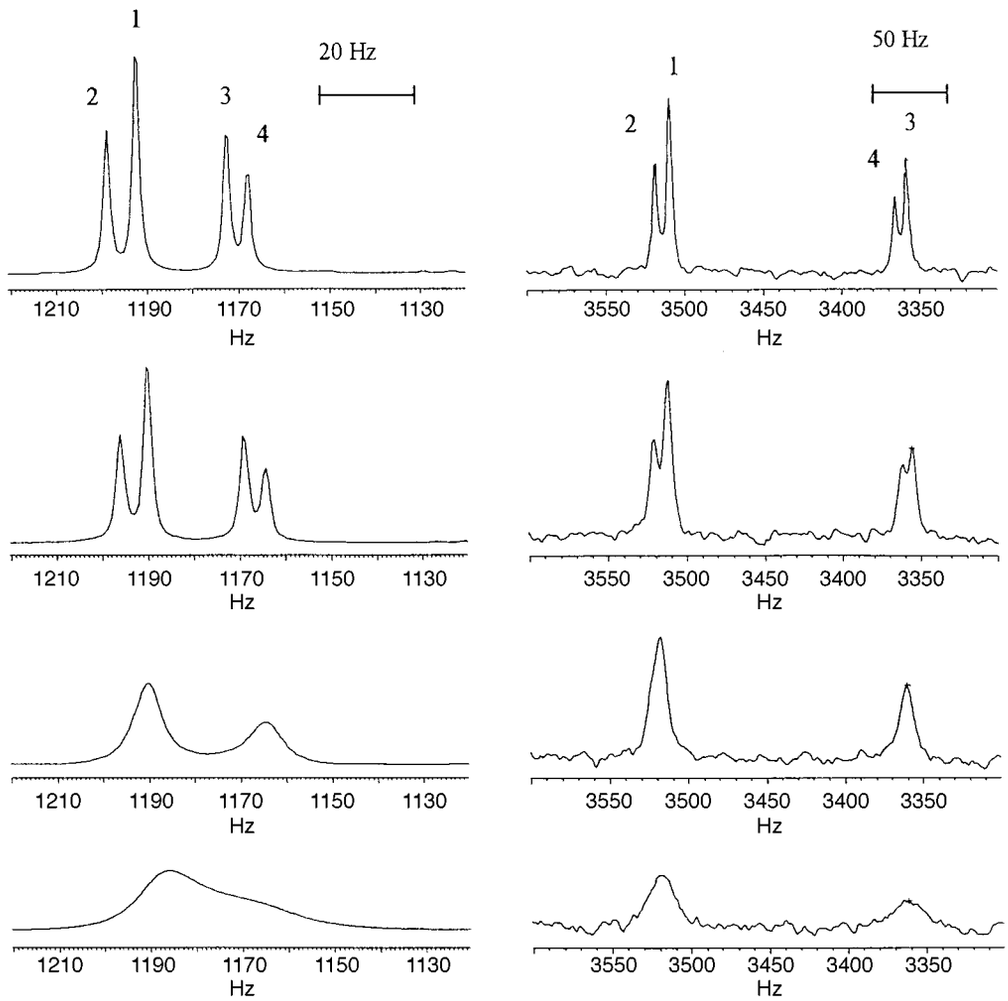

Fig. 3 ^{1}H and ^{13}C NMR spectra (left and right columns, respectively) of N–CH_3 substituents in DMDBTDMA at 10, 19.5, 44.4 and 63.1 °C (from top to bottom).

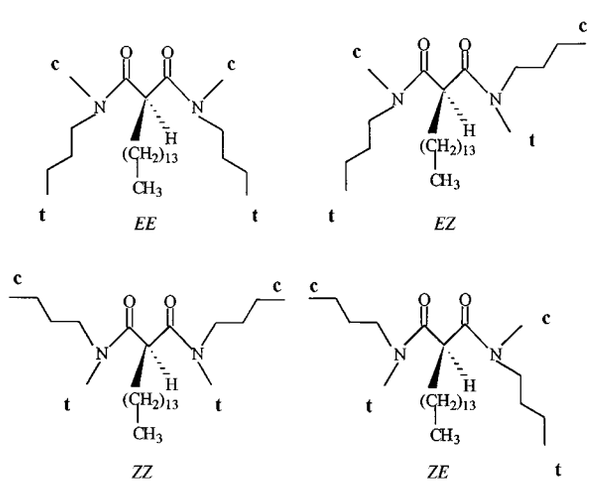

Scheme 1 Structure of the four stereoisomers *ZZ*, *ZE*, *EZ* and *EE* of DMDBTDMA together with *cis* (c) or *trans* (t) positions of N–Me and N–Bu substituents.

vents and are consequently considered as a whole in the following under a single denomination, say *ZE*. As chemical shift variations between the different isomers are small, observing separate and uncoalesced NMR patterns will depend on the solvent, temperature and working frequency. This explains the variety of experimental conditions used at this first qualitative stage of the discussion.

At temperatures slightly lower than room temperature (0–10 °C), nuclei close to the amide show splitting of their signals. This is particularly clear for N–CH_3 substituents in which both ^{1}H and ^{13}C single resonances are actually split into quartets, in fact two doublets of lines, 1 and 2 at low field, 3 and 4 at high field (Fig. 3). Both ^{1}H and ^{13}C lines: 1, 2, 3, 4 in this order have the same fractional population p_1; p_2; p_3; $p_4 = 0.38$; 0.23; 0.23; 0.16. These values depend to a small extent on the solvent and temperature; but an important feature is the strict equality of p_2 and p_3 under any circumstance. Line intensities allow us to correlate the components of both quartets to each other and to give them a common numbering. This was also confirmed by heteroscalar ^{13}C, ^{1}H correlation spectroscopy. These observations are in accord with the presence of three geometrical isomers *ZZ*, *EE* and *ZE* (Scheme 1), with an expected N–CH_3 quartet consisting of 1, 1 and 2 lines for two equivalent *trans*, two equivalent *cis*, and one *cis* and one *trans* positions, respectively. Lines 2 and 3 of equal intensity should be associated with the *ZE* isomer, each of them for either *cis* or *trans* N–CH_3 in an unknown order. Each of lines 1 and 4 are then representing either the *ZZ* or *EE* isomer. The distribution of the quartet into two sets of two closely spaced components strongly suggests that each of these doublets be assigned to either *trans* or *cis* N–CH_3 nuclei, in *ZZ* and *ZE* or *ZE* and *EE* isomers, respectively. An important problem that will be looked at in the next section is to assign *cis* and *trans* lines.

Increasing the temperature results first in a partial coalescence around 40 °C. The two doublets are transformed into two broad singlets, each of them for either *cis* or *trans* NCH_3 (in any isomer), with fractional populations $p_1 + p_2 = 0.61$ and $p_3 + p_4 = 0.39$. Above 40 °C, the two singlets in turn appear to be coalescing as in the case of a two-site exchange. At the highest

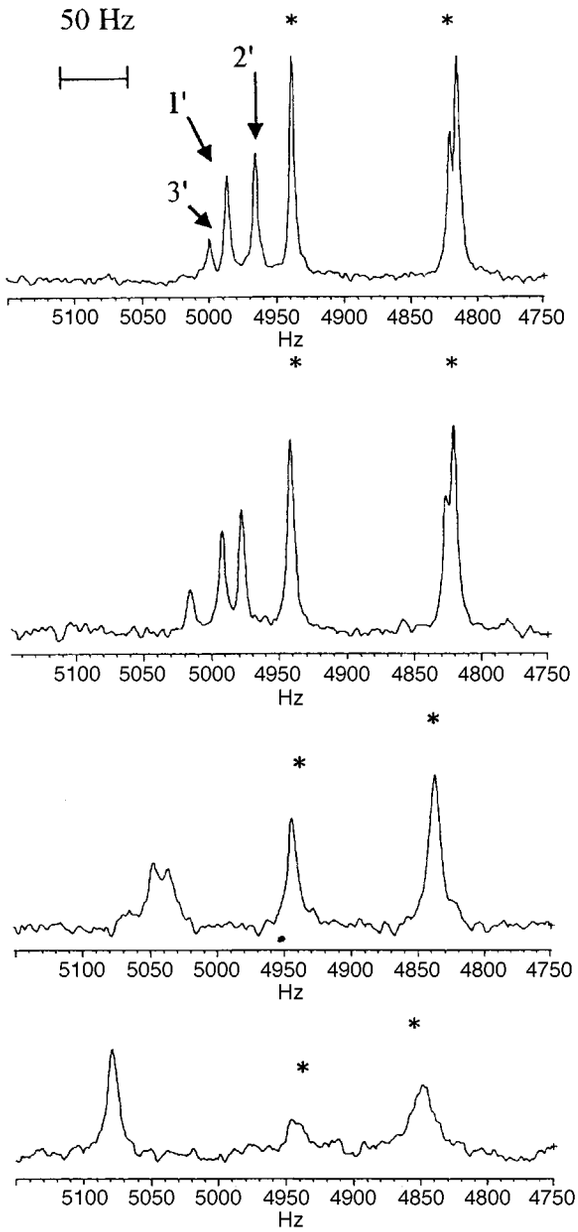

Fig. 4 ^{13}C NMR spectra of N–*C*H$_2$ (*) and *C*H fragments in DMDBTDMA at 10, 19.5, 44.4 and 63.1 °C (from top to bottom).

temperature reached in $CDCl_3$ solutions (63 °C), coalescence is nearly attained in the case of protons only, on account of a smaller chemical shift separation of ^{1}H nuclei (~40 Hz) compared to ^{13}C nuclei (~150 Hz).

These conclusions are fully confirmed by observing other nuclei in the amide structure. The carbonyl ^{13}C nuclei themselves give rise to a four line pattern at 160 ppm, exactly the same as that described above for N–CH_3 nuclei, with the same fractional populations within experimental errors (±0.01). N–CH_2 and CH carbons give rise to expected *E*,*Z* line splitting, with however some noticeable peculiarities. The expected two N–CH_2 doublets are reduced to an enlarged singlet (at low field, lines 1 and 2) and an ill-resolved doublet (at high field, lines 3 and 4), on account of small chemical shift differences between sites 1 and 2 (less than 0.5 Hz) and 3 and 4 (~4 Hz), respectively (Fig. 4). Overall fractional populations measured for each doublet are in close agreement with those mentioned above for coalesced N–CH_3 doublets (0.61 and 0.39 ± 0.01). The asymmetric methine carbon ^{13}CH gives rise to an authentic triplet (lines 1′ to 3′ in Fig. 4) since there is only one type of CH carbon in the *ZE* isomer. Fractional populations are found to be $p_2 + p_3 = 0.46$, $p_1 = 0.38$ and $p_4 = 0.16$, in this order along decreasing fields. This means that the intense high-field line represents the *ZE* isomer, and each of the other two lines either the *ZZ* or *EE* isomers. Again, CH and N–CH_2 ^{1}H spectra have similar patterns to those described in ^{13}C spectra. Due to spin–spin couplings with the adjacent methylenic protons in the tetradecyl chain, the three CH resonances appear as three ill-resolved triplets, nearly equally spaced by *ca.* 0.2 ppm, with fractional populations of 0.46 (*ZE* isomer), 0.38 and 0.16 (*ZZ* and *EE* isomers) along increasing field. N–CH_2 lines are gathered within two ill-resolved multiplets, however clearly apart from each other (by *ca.* 0.25 ppm), each of which is correlated to the two ^{13}C (unresolved and ill-resolved, respectively) doublets, with the same overall fractional populations of 0.61 and 0.39 (at high and low field, respectively). The great number of lines in each multiplet is accounted for by the magnetic non-equivalence of the two N–CH_2 protons and by geminal and vicinal ^{1}H–^{1}H spin–spin couplings.

Conformational changes other than *Z*,*E* stereoisomerism are possible within the diamide framework. Planar amide moieties can rotate about the C(O)–C(H) bond which links each of them to the methine carbon, which plays an analogous role to that of C_α carbons in peptide fragments (Scheme 2). Extending the

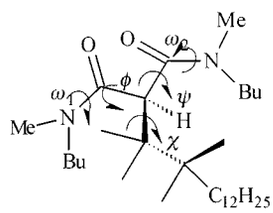

Scheme 2 Torsion angles: ϕ and ψ describing the backbone conformation in malonamides, ω_1 and ω_2 describing deviations of amide moieties from planarity, χ which characterizes the spatial arrangement of the tetradecyl side chain.

standard nomenclature used for peptides to malonamides, all possible backbone conformations can be obtained by variation of torsion angles ϕ and ψ, which measure the dihedral angles between each amide moiety and a reference molecular plane defined by the three central carbons C(O)–C(H)–C(O). Still in conformity with peptide nomenclature, we can describe deviations of the amide group from planarity by torsion angles ω_1, ω_2, and eventually characterize the spatial arrangement of the tetradecyl chain by torsion angle χ. There may exist privileged conformations minimizing the sum of internal molecular energy and solute–solvent interactions, each one with its own NMR resonances. However all these conformations should be time-averaged on the NMR timescale due to fast rotations about single bonds and thus cannot account for the observed line-splittings.

Another possibility arises from solute self-association which is known to exist in concentrated solutions of amides. In non-polar solvents, such as dodecane, tetrameric aggregates have indeed been detected by small-angle X-ray scattering.[21] Their presence is much less probable in a more polar, hydrogen-bonding solvent such as chloroform. Anyway aggregates are known to yield only time-averaged NMR spectra due to fast intermolecular exchange of individual units, a typical example is offered by micellar solutions. We can therefore again exclude this eventuality to explain NMR multiplicity in DMDBTDMA.

These two phenomena: ϕ, ψ (and eventually ω_1, ω_2, χ) angle variations and self-association, can however result in small frequency shifts in time-averaged spectra as a function of experimental conditions. The most sensitive nucleus in this view is the methine carbon, which is shifted by *ca.* 200 Hz downfield when the temperature is raised from −10 to 40 °C. This exceptional behaviour compared to that of other ^{13}C nuclei (Fig. 5) may arise from the central position of this carbon which would

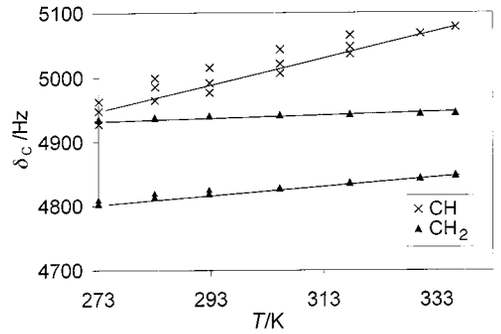

Fig. 5 ^{13}C Chemical shift variations of *C*H (triplet) and N–*C*H_2 (doublet) fragments as a function of the temperature.

make it more sensitive to the relative positions of the two amide moieties. It is however difficult from this point of view to explain why the attached methine proton is itself not subject to such exceptional variations (a few hertz only for all types of protons). An additional eventuality in this case could arise from a small contribution, *e.g.* 1%, of an enolic structure **3** on consideration of a central β-dicarbonyl arrangement in DMDBTDMA.

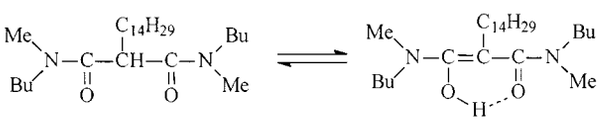

1 **3**

Assuming time-averaged-spectra for both ^{13}C and ^{1}H nuclei, and intrinsic chemical shift variations of about 50 ppm (*i.e.* 20000 Hz) and 1 ppm (*i.e.* 400 Hz) for the ethylenic carbon and the hydroxylic proton in **3**, would then lead to average frequency shifts of *ca.* 200 and 4 Hz, respectively, which have indeed a correct order of magnitude. Whatever their origin, these frequency shifts are to be taken into consideration in lineshape calculations of variable-temperature NMR spectra (see later).

Assignment of NMR signals

A proper assignment of NMR signals is important in the case of unsymmetrical *N*-disubstituted amides such as DMDBTDMA since it serves to identify the *Z*, *E* isomers shown in Scheme 1. Conclusive experiments generally used for this purpose are the inequality of *cis*, *trans* vicinal couplings and of the intramolecular Overhauser effect. They cannot be worked out in the present case due to multiple *N*- and *C*-substitution. The *cis* (c) or *trans* (t) position of *N*-methylic protons in either the *EE* (cc) and *ZE* (tc) isomers or the *ZE* (tc) and *ZZ* (tt) isomers, respectively, was assigned to high-field or low-field doublets (Fig. 3), respectively, on the following grounds.

First, a review of the literature[1] indicates that when the R–C(O) substituent in a monoamide is larger than hydrogen, the bulkier *N*-substituent is preferably *cis* to the carbonyl oxygen, as a consequence of the size of the relevant groups decreasing along the sequence R > CH_3 > O > H.[33] By analogy, the most abundant N–CH_3 doublet (61%) in DMDBTDMA is to be assigned to *trans* (t) N–CH_3 protons, *i.e.* to the *ZZ* isomer and the *Z* end of the *ZE* isomer. We confirmed this presumption by two series of experiments using either Aromatic Solvent Induced Shifts (ASIS)[34] or Lanthanide Induced Shifts (LIS).[35]

ASIS experiments. A criterion generally accepted for signal assignment is that the resonance absorption belonging to *N*-alkyl protons *trans* to the carbonyl oxygen in amides is shifted farther upfield than the *cis* protons by going from a non-aromatic to an aromatic solvent like benzene.[36] This shielding effect is traced to the existence of (i) benzene–solute associ-

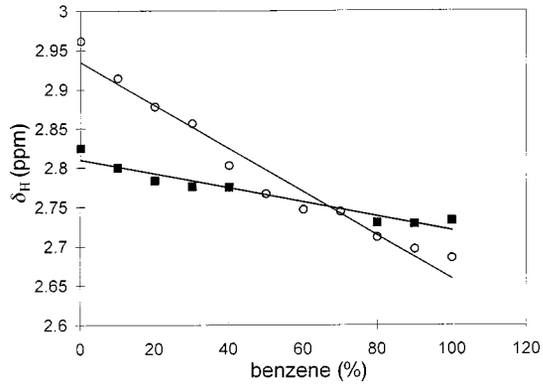

Fig. 6 ^{1}H Chemical shift variations of *Z* (○) and *E* (■) isomers in ASIS experiments: plots of δ(N–CH_3) *vs.* the benzene content in C_6H_6–dodecane-d_{26} solvent mixtures at 25 °C.

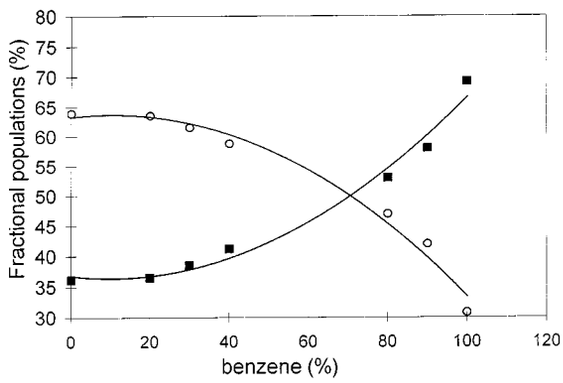

Fig. 7 Fractional populations of *Z* (○) and *E* (■) isomers in ASIS experiments measured from N-CH_3 ^{1}H doublets.

ations, and (ii) the ring-current field shifting upfield amide nuclei located within the benzene magnetic anisotropy cone along the C_6-symmetry axis. The larger upfield shift of the *trans* protons was assigned to a specific interaction between the π electrons of benzene and the positively charged amide nitrogen (*cf.* resonance structure **2**), with the negatively charged carbonyl oxygen being as far away from the benzene ring as possible. We used in this respect 0.5 molar DMDBTDMA solutions in a series of benzene–dodecane mixtures at 25 °C. Chemical shifts of low- and high-field lines (centres of the two ill-resolved doublets) were measured as a function of the benzene volume percentage in the solvent mixture. The graphs thus obtained (Fig. 6) are approximately straight lines with clearly different slopes. The low-field more intense doublet observed in dodecane-d_{26} or chloroform-d is associated with the greatest slope, and should then be assigned to *trans N*-methylic protons, *i.e.* lines 1 and 2 (see above), in *ZZ* and *ZE* (*Z* end only) isomers. Similarly, the high field weaker doublet represents *cis* N–CH_3 protons in the *ZE* and *EE* isomers, lines 3 and 4, respectively. On increasing the volume fraction of benzene over *ca.* 60%, the *cis* and *trans* doublets interchange (i) their relative positions on the chemical shift scale, the *cis* N–CH_3 protons thus appearing at lower field than the *trans* protons (Fig. 6), and (ii) their fractional population (Fig. 7), the amide *cis*/*trans* equilibrium being itself shifted as a consequence of energetically favoured solute–solvent interactions in the *E* isomers. The overall NMR pattern is thus deceptively similar in both aromatic and non-aromatic solvents, with opposite line assignments in the two media. ^{13}C N–CH_3 lines were assigned in turn either by consideration of ^{1}H and ^{13}C fractional populations or by heteroscalar ^{13}C–^{1}H correlation spectroscopy. Finally the *cis* and *trans* N–CH_2 and CH resonances are easily identified from line intensities.

LIS experiments. Addition of lanthanide shift reagents

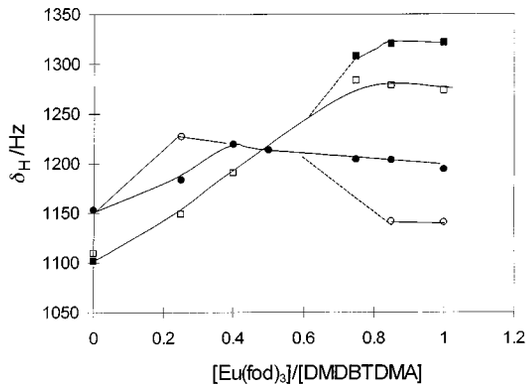

Fig. 8 ^{1}H Chemical shift variations of *trans* and *cis* N–CH_3 substituents in *ZZ* (●), *ZE* (○) and EZ (□), EE (■) isomers, respectively, in LIS experiments.

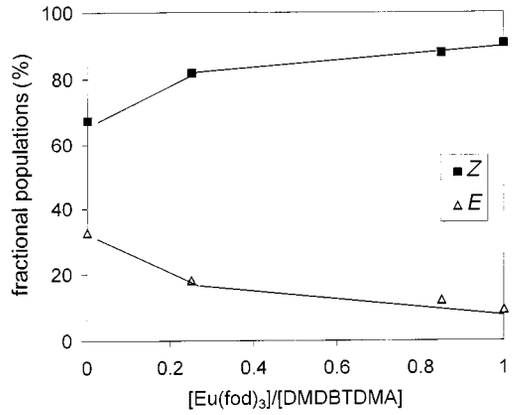

Fig. 9 Fractional populations of *Z* and *E* conformations in LIS experiments.

(LSR), such as Eu(fod)$_3$, to CCl_4 solutions of dimethylformamide (DMF) induces differential downfield shifts $\Delta\delta(cis) > \Delta\delta(trans)$ of *cis* and *trans* N–CH_3 ^{1}H signals.[37] Plots of $\Delta\delta$ as a function of the ratio ρ = [Eu(fod)$_3$]:[amide] have initial ascending slopes larger for *cis* than for *trans* N–CH_3 protons of DMF, a fact that could be used as a criterion for stereochemical assignments in unsymmetrically *N*-substituted amides. In the presence of excess reagent ($\rho \geq \sim 1$), $\Delta\delta$ has a limiting value Δ_i, which represents the intrinsic shift induced in amide molecules fully associated to LSR. The fact that Δ_i (*cis*) is larger than Δ_i (*trans*) can also be used as a criterion to distinguish between *cis* and *trans* N–CH_3 substituents. This second criterion is even more reliable than considering the initial slopes since, in the absence of an excess of reagent, the fraction of associated amide may happen to be smaller in the intrinsically more shifted isomer, this may give rise in turn to inversions in the initial magnitudes of $\Delta\delta$ (*cis*) and $\Delta\delta$ (*trans*). Such a situation, already described in the literature for secondary amides,[38] also prevails with 0.15 molar solutions of DMDBTDMA in CCl_4 at 20 °C, used in our investigations. Apparent chemical shift variations are of similar (or even in an opposite order to what is expected) size for all four *Z*,*E* isomers as long as $\rho \leq \sim 0.5$, and then are clearly larger for the two components of the high-field N–CH_3 doublet than for those of the low-field doublet (Fig. 8). The latter observation is indeed in line with our previous assignment of the low-field (lines 1 and 2) and high-field (lines 3 and 4) doublets to *cis* (*ZZ* and *ZE* isomers) or *trans* (*EE* and *ZE* isomers), respectively. As in the case of ASIS experiments, introducing an extraneous chemical probe to test the presence of conformers can greatly perturb the *Z*:*E* isomer ratio. This event has already been reported in the literature with secondary amides such as *N*-methylformamide.[38] In the present investigations, the fractional population of the *trans* N–CH_3 low-field doublet increases from 67% in pure CCl_4 (instead of 61% in $CDCl_3$) to 91% upon addition of an equimolar amount of Eu(fod)$_3$ (Fig. 9), at the expense of the *cis* high-field doublet, which consequently decreases from 33% to 9%.

Barriers to rotation

Kinetic scheme for internal rotations. These geometrical isomers *ZZ*, *ZE* and *EE* of DMDBTDMA exist in equilibrium in $CDCl_3$ at 25 °C, with fractional populations p_{ZZ}, p_{ZE} and p_{EE} = 0.38, 0.46 and 0.16, respectively. Synchronous torsional rotations of both amide moieties can be rejected since the formation of geared systems requires strong steric interactions between correlated fragments.[39] This means that equilibration $ZZ \rightleftharpoons EE$ between the all *cis* and all *trans* isomers can only occur through two consecutive equilibria, $ZZ \rightleftharpoons ZE$ and then $ZE \rightleftharpoons EE$, as shown in Scheme 3(a). In the same way, equilibration between the two enantiomers $ZE \rightleftharpoons EZ$, which interchanges *Z* and *E* nuclei in the geometrical

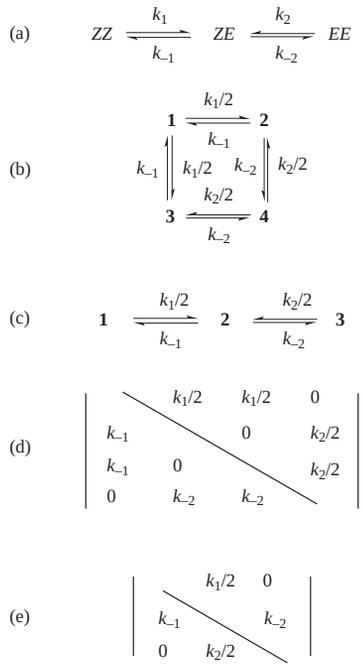

Scheme 3 Chemical exchanges in DMDBTDMA (a) with the accompanying NMR site exchanges in the four-line (b) or three-line (c) NMR patterns (see the text) and the corresponding exchange matrices (d and e, respectively).

isomer "*ZE*", is carried out through the same sequence of equilibria.

Two equilibrium constants, K_1 and K_2, and four rate constants k_1, k_{-1}, k_2 and k_{-2} are required to describe this set of consecutive conformational changes [eqn. (1)]. These two

$$K_1 = k_1/k_{-1} = p_{ZE}/p_{ZZ} \text{ and } K_2 = k_2/k_{-2} = p_{ZE}/p_{EE} \quad (1)$$

chemical exchanges induce nuclear magnetization transfers, the so-called nuclear site exchange. This was observed in the present case, simultaneously and independently, on four types of nuclei, the N–CH_3 protons, the N–CH_3, N–CH_2 and CH carbons. Each of the first three nuclei undergoes a four-site exchange between lines 1 to 4 composing their NMR spectrum (see above), with fractional populations in each site, $p_1 = p_{ZZ}$, $p_2 = p_3 = p_{ZE}/2$, $p_4 = p_{EE}$. Pathways for site exchange are shown in Scheme 3(b), together with the corresponding exchange matrix, Scheme 3(d).[40] Exchanges between sites 1 and 4 on the one hand, and 2 and 3 on the other hand, are forbidden for the reasons given in the above paragraph. Exchange probabilities from site 1 to 2 or 3 (or from site 4 to 2 or 3) are half the corresponding chemical rate constant k_1 (or k_2), because one individual *Z* (or *E*) moiety over two in *ZZ* (or *EE*) isomer is

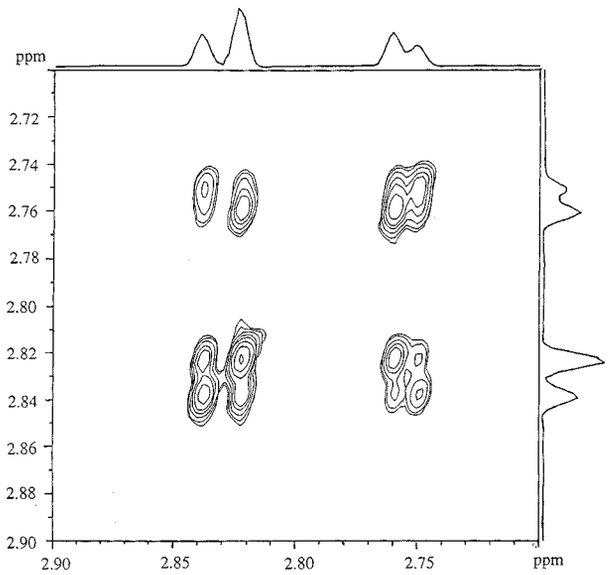

Fig. 10 ^{1}H 2D EXSY spectrum of DMDBTDMA in $CDCl_3$ at 20 °C showing the N–CH_3 region only. Assignments are given according to the *cis* (c) or *trans* (t) positions of the two N–CH_3 substituents with respect to carbonyl oxygen (see the text).

converted into an *E* (or *Z*) moiety in the *ZE* isomer (whether the enantiomer is *ZE* or *EZ*). Non-zero off-diagonal elements in the exchange matrix [Scheme 3(d)] are then $k_1/2$, $k_2/2$, k_{-1} and k_{-2}.

Two dimensional NMR (EXSY)[25,26] was used to test the validity of the proposed kinetic pathways. In this method, magnetization transfers correlating pairs of sites in mutual exchange are visualized by observing cross-peaks at the corresponding pairs of lines appearing on both the vertical and the horizontal frequency scale ω_1,ω_2. Ideally, cross-peaks provide a graphical projection of the exchange matrix. In reality, there may also exist "indirect" cross-peaks due to magnetization transfers arising from sequential processes in multisite systems as those studied presently. However indirect magnetization transfers are occurring late in the course of the pulse sequence. Indirect cross-peaks are thus much less intense than direct cross-peaks, especially in experiments using mixing times t_m as short as possible, and are generally easily recognized as parasitic spots in the 2D spectrum. In the present case (Fig. 10), one may observe the absence of cross-peaks connecting lines 1 and 4 on the one hand, and 2 and 3 on the other hand, as expected. This is particularly clear on the upper half of the spectrum (above the diagonal), while some parasitic weak indirect cross-peaks are somewhat obscuring the contour plots below the diagonal. To conclude, this EXSY experiment significantly contributes to putting the kinetic Schemes 3(a) and 3(b) on a firm basis.

As mentioned in the previous section, the two doublets which constitute the four-site NMR spectrum presently studied can be reduced to two broadened singlets in the case of nearly zero chemical shift separation or of partial coalescence at temperatures above *ca.* 40 °C. If we assume a perfect coincidence of line frequencies within the two doublets, we may consider that we are dealing with an overall two-site exchange [reaction (2)],

$$Z \underset{k_{EZ}}{\overset{k_{ZE}}{\rightleftharpoons}} E \qquad (2)$$

as the result of chemical exchange between amide moieties in the *Z* or *E* conformation whatever the isomer. Fractional populations of sites *Z* and *E* are $p_Z = p_{ZZ} + p_{EZ}/2$ (= 0.61 in $CDCl_3$) and $p_E = p_{EE} + p_{EZ}/2$, respectively.

Apparent overall rate constants k_{ZE} and k_{EZ} are easily related to individual rate constants k_1, k_2 according to eqn. (3). Two conclusions may be drawn at this point. First, a two-site treatment results in apparent rate constants which may be far from the true individual values k_1, k_2, *e.g.* k_{ZE}, k_{EZ} = 11.8 and 18.4 s^{-1} when k_1, k_2 = 17 and 50 s^{-1} at 40 °C. Second, and more importantly, the complete four-site treatment presumably approaches a degenerate two-site exchange behaviour at higher temperatures. This means that only a weighted mean of the rate constants k_1, k_2, as shown in eqn. (3), can be ultimately obtained from lineshape analysis; in other words, the standard four-site treatment is likely to have extended uncertainty ranges in k_1, k_2 adjustments under these conditions.

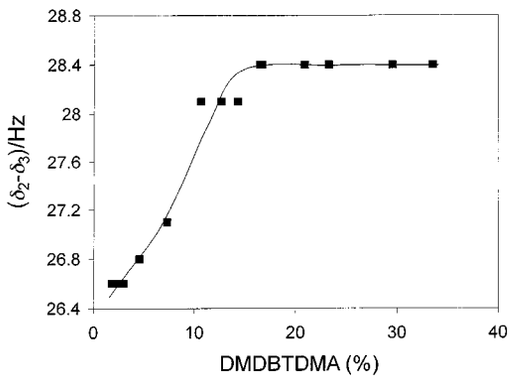

Fig. 11 ^{1}H Chemical shift differences ($\delta_2 - \delta_3$) between N–CH_3 lines 2 and 3 as a function of weight percentage of DMDBTDMA in $CDCl_3$ solution at 25 °C.

$$p_Z k_{ZE} = p_E k_{EZ} = p_1 k_1/2 + p_4 k_2/2 \qquad (3)$$

Lineshape analysis of the CH three-site NMR pattern is especially valuable in this respect. Sites 1′, 2′, 3′ stand for each of the three isomers, *ZZ*, *ZE* and *EE*, with populations $p_{1'} = p_{ZZ}$, $p_{2'} = p_{ZE}$ and $p_{3'} = p_{EE}$. Nuclear site exchange, described by a 3 × 3 exchange matrix [Scheme 3(c) and 3(e)], has the same rate constants as chemical exchange itself. Lines 1′ to 3′ (Fig. 4) are relatively far from each other, and nearly equally spaced, in which case chemical exchange cannot result in a deceptive two-site like behaviour at high temperatures.

Lineshape analysis. DNMR patterns of multisite exchanges are complex since coalescence is generally occurring progressively between various pairs of lines (Figs. 3 and 4). This has two consequences, (i) the NMR window may extend over a wide range of temperature, between *ca.* 30 and 65 °C in the present case, *i.e.* over 35 °C, instead of *ca.* 20 °C for two-site exchanges in simple monoamides, this results in more reliable Arrhenius activation energies, and (ii) curve-fitting over a great number of lines permits a more precise adjustment of unknown rate constants, this is valuable in the present case where two rate constants k_1, k_2 (instead of one for monoamides) are required in the kinetic Scheme 3. It should be recalled that obtaining reliable values for barriers to rotation in simple monoamides, such as dimethylformamide or *N*-methylformamide, has proved to be a difficult task, because the chemical shift difference between the two exchanging lines is generally small and subject to changes with concentration, solvent and temperature.[1b]

Chemical shift differences ($\delta_2 - \delta_3$) between the two ^{1}H doublets (more precisely, between lines 2 and 3) of the uncoalesced N–CH_3 spectrum as a function of the weight fraction of DMDBTDMA in $CDCl_3$ at 25 °C are represented in Fig. 11. ($\delta_2 - \delta_3$) increases from 26.6 to 28.4 Hz, and then remains approximately constant, when the amide content is raised up to *ca.* 15%, and more, respectively. As for those already described for ^{13}C nuclei (Fig. 5), these variations are likely to proceed, in an unknown manner, from the combined effects of self-association, solute–solvent interactions and conformational changes. NMR operations were performed for this reason at a constant weight percentage of 17%, *i.e.* in 0.5 molar solutions. Another reason for that is a progressive increase of rate con-

Table 2 Variable-temperature forward rate constants k_1, k_2 for internal rotation in the *ZZ* and *EE* isomers of DMDBTDMA in $CDCl_3$ solutions, and the derived activation parameters at 25 °C, with estimated errors, for each of four NMR patterns

	N–CH_3	N–CH_3	N–CH_2	CH
k_1 (305.1 K)/s^{-1}	5	6	5	3
k_2 (305.1 K)/s^{-1}	10	18	15	6
k_1 (317.6 K)/s^{-1}	17	20	10	12
k_2 (317.6 K)/s^{-1}	50	50	30	36
k_1 (330.1 K)/s^{-1}	43	40	40	35
k_2 (330.1 K)/s^{-1}	130	120	120	105
k_1 (336.3 K)/s^{-1}	75	60	60	65
k_2 (336.3 K)/s^{-1}	225	150	180	195
$\Delta H_1^{\ddagger}$/kJ mol^{-1}	70.4 ± 2.2	59.3 ± 3.2	68.4 ± 8.0	80.5 ± 2.3
$\Delta S_1^{\ddagger}$/J K^{-1} mol^{-1}	−0.5 ± 6.9	−35.0 ± 14.9	−8.6 ± 25.0	28.3 ± 7.0
$\Delta G_1^{\ddagger}$/kJ mol^{-1}	70.6 ± 0.2	69.7 ± 0.3	70.9 ± 0.6	72.1 ± 0.2
$\Delta H_2^{\ddagger}$/kJ mol^{-1}	81.2 ± 6.1	56.7 ± 2.7	68.4 ± 8.1	91.0 ± 6.6
$\Delta S_2^{\ddagger}$/J K^{-1} mol^{-1}	41.1 ± 18.9	−34.6 ± 11.4	0.5 ± 25.0	69.3 ± 20.7
$\Delta G_2^{\ddagger}$/kJ mol^{-1}	68.9 ± 0.4	67.0 ± 0.3	68.2 ± 0.6	70.4 ± 0.5

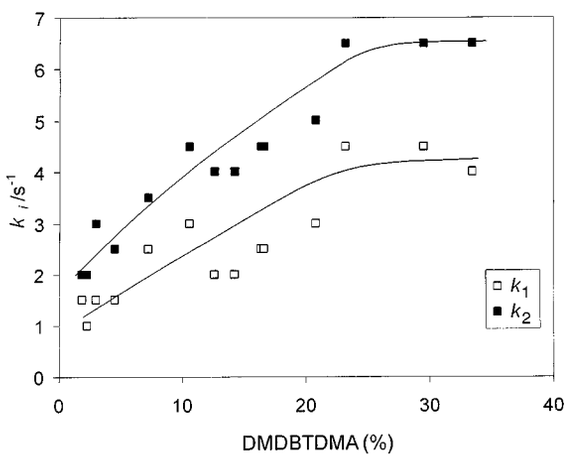

Fig. 12 Rate constants k_1, k_2 for conformational changes *ZZ*→*ZE* and *EE*→*ZE*, respectively, as a function of weight percentage of DMDBTDMA in $CDCl_3$ solution at 25 °C.

stants k_1, k_2 themselves as a function of the amide content as shown in Fig. 12. Besides concentration effects, all lines are slightly shifted upfield or downfield with the temperature as long as they can be observed before coalescence. As lineshape computations require the knowledge of exact frequencies δ_i of the exchanging sites i, we proceeded first to a rough extrapolation of δ_i at high temperature from the values measured at lower temperature, and then to the final adjustment of δ_i values in the last steps of the least squares procedures used to estimate k_1 and k_2. The knowledge of the fractional populations p_i of sites in mutual exchange is also required for calculation of lineshapes and of the rate constants k_{-1}, k_{-2} according to eqn. (1). In the case of monoamides[1] and polypeptides,[13] p_i values generally remain constant within experimental errors over the temperature range for DNMR experiments, revealing equilibrium enthalpies $\Delta H°$ close to zero. This is the case for DMDBTDMA, where constant values of p_i (within ±0.01, see the preceding section) are measured below coalescence, from 0 to 30 °C, with corresponding equilibrium enthalpies ΔH_1^0 and $\Delta H_2^0 = 0 \pm 1$ kJ mol^{-1} and free energies ΔG_1^0 and $\Delta G_2^0 = -473$ and −2616 J mol^{-1} at 25 °C.

DNMR experiments were performed at four temperatures, 32.2, 44.4, 56.9 and 63.1 °C in a single solvent ($CDCl_3$). Rate constants k_1, k_2 were determined using four NMR patterns as explained above. Arrhenius activation energies $E^{\ddagger}$ and frequency factors A were determined from a least-squares analysis of Arrhenius plots for each NMR pattern for the sake of comparison. Activation enthalpies, entropies and free energies were deduced from Arrhenius parameters A and E, and the least-squares rate constant k at temperature T according to Eyring equations. Their numerical expression using SI units is[40] given in eqn. (4). The whole set of data is displayed in Table 2. The

$$\Delta H^{\ddagger}(\text{J mol}^{-1}) = E^{\ddagger} - 8.314T$$
$$\Delta S^{\ddagger}(\text{J K}^{-1}\text{ mol}^{-1}) = 19.143 \log (A/T) - 205.8 \quad (4)$$
$$\Delta G^{\ddagger}(\text{J mol}^{-1}) = \Delta H^{\ddagger} - T\Delta S^{\ddagger} = 19.143T[10.318 - \log(k/T)]$$

agreement between the sets of four rate constants k_1 or k_2 measured at each temperature (at the top of the table) is relatively good at high temperature (by *ca.* ±10%) and becomes poor at lower temperatures, this results from a higher sensitivity of spectra far from coalescence to erratic chemical shift and/or temperature variations or to field inhomogeneity. Least squares analyses of Arrhenius plots result for each NMR pattern in $\Delta H_i^{\ddagger}$, $\Delta S_i^{\ddagger}$, $\Delta G_i^{\ddagger}$ ($i = 1$ or 2) values with relatively narrow uncertainty ranges. However the comparison between the four series of activation parameters shows that they are mutually compatible within the uncertainty range computed for each of them only in the case of $\Delta G_i^{\ddagger}$ values, while activation enthalpies or entropies differ from each other well beyond the stated individual error margins. This shows the difficulty of obtaining reliable barriers to rotation in amides from a single series of experiments. This has already been noticed with monoamides, *e.g.* values given in the literature for Arrhenius activation energy in dimethylformamide[1b] range between 52 and 234 kJ mol^{-1}. In the present case we can greatly improve the reliability of announced kinetic parameters by averaging the results over the four series of measurements. This is carried out (Table 3) in either of two ways: (a) as arithmetic means of $\Delta H_i^{\ddagger}$, $\Delta S_i^{\ddagger}$, $\Delta G_i^{\ddagger}$

Table 3 Rate constants and activation parameters at 25 °C for the forward and reverse reactions in conformational equilibria (1) *ZZ* ⇌ *ZE* and (2) *EE* ⇌ *ZE*. A comparison between values computed as arithmetic means over four NMR patterns (a) or from least-squares analysis over the whole set of 16 experimental points (b)

	k_1/s^{-1}	k_{-1}/s^{-1}	k_2/s^{-1}	k_{-2}/s^{-1}
(a)	2.5 ± 0.5	2.0 ± 0.4	6.3 ± 1.7	2.2 ± 0.6
(b)	2.5 ± 0.6	2.1 ± 0.5	6.1 ± 1.9	2.1 ± 0.6
	$\Delta H_1^{\ddagger}$/ kJ mol^{-1}	$\Delta S_1^{\ddagger}$/ J K^{-1} mol^{-1}	$\Delta G_1^{\ddagger}$/ kJ mol^{-1}	$\Delta G_{-1}^{\ddagger}$[c]/ kJ mol^{-1}
(a)	69.6 ± 4.4	−3.9 ± 13	70.8 ± 0.5	71.3 ± 0.5
(b)	66.9 ± 4.5	−12.6 ± 14.0	70.6 ± 0.6	71.1 ± 0.6
	$\Delta H_2^{\ddagger}$/ kJ mol^{-1}	$\Delta S_2^{\ddagger}$/ J K^{-1} mol^{-1}	$\Delta G_2^{\ddagger}$/ kJ mol^{-1}	$\Delta G_{-2}^{\ddagger}$[c]/ kJ mol^{-1}
(a)	74.3 ± 7.5	19.1 ± 22.8	68.6 ± 0.7	71.2 ± 0.7
(b)	72.5 ± 5.5	13.4 ± 17.2	68.5 ± 0.8	71.1 ± 0.8

[c] Computed as $\Delta G_{-i}^{\ddagger} = \Delta G_i^{\ddagger} - \Delta G_i^0$.

and k_i (298.15 K) (estimated rate constant at 25 °C) values over the four NMR patterns, or (b) from an overall least-squares analysis over the whole set of sixteen experimental points. It can be seen that the two averaging procedures yield coherent series of numbers, close to each other with overlapping error margins. The values for free energies of activation can be given with a high degree of confidence, $\Delta G_1^{\ddagger} = 70.7 \pm 0.5$ and $\Delta G_2^{\ddagger} = 68.5 \pm 0.5$ kJ mol^{-1}. We also report in Table 3 rate constants k_{-i} for reverse reactions, computed according to eqn. (1), and the corresponding free energies of activation from eqn. (5).

$$\Delta G_{-i}^{\ddagger} = \Delta G_i^{\ddagger} - \Delta G_i^{0} \quad (5)$$

Activation enthalpies $\Delta H_i^{\ddagger}$ can be given with uncertainty ranges of *ca.* ±5 kJ mol^{-1} with values of 68 and 73 kJ mol^{-1} ($i = 1$ or 2, respectively), while activation entropies are zero within estimated error, $\Delta S_i^{\ddagger} = 0 \pm 20$ J K^{-1} mol^{-1}.

Free energies of activation have an order of magnitude similar to that observed in *N*,*N*-disubstituted monoamides, RC(O)NR′R″, where barriers to rotations are lowered by the steric requirements of R, R′, R″ destabilizing the ground state (by causing deviations from planarity of the amide system), *e.g.* with R′ = R″ = CH_3, $\Delta G^{\ddagger} = 72.4$ and 72.8 kJ mol^{-1} in CCl_4 for R = CH_3 [41] or CH_3CH_2,[42] respectively. Most studies of amides in solution indicate an entropy of activation close to zero, as is also observed in DMDBTDMA. Our results show an overall behaviour of each amide moiety in DMDBTDBMA quite similar to that in simple monoamides, this points to an absence of large mutual effects between the two amide moieties over the barriers to rotation.

There are however slight differential effects: the rotation of one *N*-butyl substituent from a *cis* (*Z*) to a *trans* (*E*) position is somewhat faster when its companion in the adjacent amide moiety is in the *E* rather than the *Z* position. This amounts to comparing the basic *Z* to *E* interchange in the *ZE* and *ZZ* isomers, respectively, with the results: k_{-2} (2.2 s^{-1}) > $k_1/2$ (1.25 s^{-1}). Conversely the reverse reaction $E \rightarrow Z$ is faster in the *EE* than in the *ZE* isomer, with $k_2/2$ (3.15 s^{-1}) > k_{-1} (2.1 s^{-1}). Along the same lines, these differential effects fortuitously result in an approximate equality of reverse reaction rates k_{-1} and k_{-2}, as the consequence of (i) decreasing the $E \rightarrow Z$ rate constants from $k_2/2$ to k_{-1} on starting from the *EE* or *EZ* isomers, respectively, and of (ii) increasing the $Z \rightarrow E$ rate constants from $k_1/2$ to k_{-2} on starting from the *ZZ* or *ZE* isomers, respectively. The fact that the latter values are modified in about the same ratio, 1.5 and 1.7 respectively, shows that the structural effects seem to obey approximately linear free energy relationships.

Concerning the origin of these effects, the neighbouring amide moiety in a given isomer may bring stabilizing/destabilizing energy to either the ground state or the transition state in the rotational process occurring in its companion moiety. An indication that the ground state energy in each amide moiety is independent of the *Z* or *E* state of the adjacent moiety is the statistical nature of the distribution of the *ZZ*, *ZE* and *EE* stereoisomers. This means that if we consider the overall population of *Z* and *E* units in DMDBTDMA, $p_Z = 0.61$ and $p_E = 0.39$ (see above), a random distribution of these units two by two among DMDBTDMA stereoisomers is observed according to probability laws [eqn. (6)].

$$p_{ZZ} = p_Z p_Z;\ p_{\text{“}ZE\text{”}} = p_{ZE} + p_{EZ} = 2p_Z p_E \text{ and } p_{EE} = p_E p_E \quad (6)$$

Another indication supporting this view is the above-mentioned contribution of these structural effects to the reverse reaction rates k_{-1} *and* k_{-2}, in which case both $E \rightarrow Z$ and $Z \rightarrow E$ rotations have a common ground state. Differences in rate constants should then arise from destabilization of the transition state by an adjacent *Z* butyl substituent (compared to an *E* substituent). The reason for such a destabilization is not clear. A direct effect would involve a steric inhibition of mesomerism in the transition state for an unknown reason. An indirect effect could involve stabilization of the transition state through weak hydrogen-bonding of the negatively charged carbonyl oxygen to chloroform. The differential effect on rate constants would arise from steric requirements induced by the presence of bulky *N*-butyl substituents in the position *cis* to the carbonyl. A detailed study of solvent effects on rotational barriers would be necessary to try and elucidate this point.

Conclusion

Weak mutual interactions do exist between the two amide moieties of DMDBTDMA, this allows us to observe three geometrical isomers, in slow exchange on the NMR timescale. These isomers were identified on the basis of ASIS and LIS experiments. Fractional populations obey simple probability laws, so that only one parameter p_Z (or $p_E = 1 - p_Z$) is required to compute them. The kinetic scheme (Scheme 3) involves four types of conformational changes and therefore four rate constants, two of them are independent; in this way, three parameters are sufficient to describe the system at one temperature, p_Z, k_1, k_2. The bulkiness of substituents on nitrogens and the central carbon lowers the barriers to rotation to values similar to those obtained with substituted monoamides. The presence of a long alkyl chain does not seem to bring any peculiar behaviour. The simultaneous presence of two amide units in the propane-1,3-diamide framework of DMDBTDMA slightly modifies barriers to rotation according to the nature of conformers: reaction rates for both $E \rightarrow Z$ and $Z \rightarrow E$ conformational changes in an amide moiety are decreased by a factor of *ca.* 1.5 when its companion moiety assumes a *Z* rather than an *E* conformation.

Acknowledgements

The authors wish to thank GDR (Groupement de Recherche) PRACTIS, which was at the origin of this work. The group at Nancy wishes also to thank E. Dumortier (UMR 7565 UHP Nancy) for his help with computer work, E. Eppiger and P. Mutzenhardt (Service Commun de RMN—UHP Nancy) for the acquisition of the NMR experimental data, C. Charbonnel and X. Heres (CEA/SEMP, Marcoule) for the gifts of DMDBTDMA. Lydie Lefrançois is indebted to EDF for the financial support to her thesis. Work at the CEA was partially financed by COGEMA, EDF and by the European Commission under the 4th PCRD “Nuclear Fission Safety” programme (Contract F 96010).

References

1 For a review, see (*a*) W. E. Stewart and T. H. Siddall, III, *Chem. Rev.*, 1970, **70**, 517; (*b*) G. Binsch, *Top. Stereochem.*, 1968, **3**, 97; (*c*) M. Oki, *Applications of Dynamic NMR Spectroscopy to Organic Chemistry*, VCH, Deerfield Beach, FL, 1985, p. 43.
2 L. Pauling, *The Nature of the Chemical Bond*, Cornell University Press, Ithaca, NY, 1960, p. 281.
3 W. D. Phillips, *J. Chem. Phys.*, 1955, **23**, 1363.
4 H. S. Gutowsky and C. H. Holm, *J. Chem. Phys.*, 1956, **25**, 1228.
5 C. Berthon and C. Chachaty, *Solvent Extr. Ion Exch.*, 1995, **13**, 781.
6 K. Wüthrich, *NMR in Biological Research: Peptides and Proteins*, North Holland, Amsterdam, 1976, pp. 73 and 184.
7 E. A. Noe and M. Raban, *J. Am. Chem. Soc.*, 1975, **97**, 5811.
8 E. A. Noe and M. Raban, *J. Am. Chem. Soc.*, 1974, **96**, 1598.
9 G. J. Bishop, B. J. Price and I. O. Sutherland, *J. Chem. Soc.*, *Chem. Commun.*, 1967, 672.
10 C. Berthon, *Thèse de l'Université Blaise Pascal-Clermont II*, 1993. CEA-R 5644.
11 C. Berthon, F. Vaufrey, J. Livet, C. Madic and M. J. Hudson, *Proceedings of the ISEC'96*, Melbourne, Australia, 1996, vol. 2, pp. 1349.
12 J. Chrisment, J.-J. Delpuech and W. Rajerison, *J. Chim. Phys.*, 1991, **88**, 1757.
13 J. Chrisment and J.-J. Delpuech, *Langmuir*, 1996, **12**, 2441.
14 D. A. Torchia and J. R. Lyerla, *Biopolymers*, 1974, **13**, 97.

15 M. Bourgeois, in *Techniques de l'Ingénieur*, *Traité Mécanique et Chaleur*, ISTRA BL, Shiltigheim, 1994, vol. B 3650, p. 1.
16 C. Madic, P. Blanc, N. Condamines and N. Baron, *Proceedings of the International Conference on Nuclear Fuel Reprocessing and Waste Management*, *RECOD'94*, London, 1994, vol. 3.
17 L. Nigond, N. Condamines, P. Y. Cordier, J. Livet, C. Madic, C. Cuillerdier, C. Musikas and M. J. Hudson, *Sep. Sci. Technol.*, 1995, **30**, 2075.
18 L. Nigond, C. Musikas and C. Cuillerdier, *Solvent Extr. Ion Exch.*, 1994, **12**, 261.
19 L. Nigond, C. Musikas and C. Cuillerdier, *Solvent Extr. Ion Exch.*, 1994, **12**, 297.
20 (*a*) European report EUR 18038 (1998); (*b*) C. Madic, M. J. Hudson, J. O. Liljenzin, J. P. Glatz, R. Nannicini, A. Facchini, Z. Kolarik and R. Odot, *Proceedings of the 5th International Information Exchange Meeting on Actinide and Fission Product Partitioning and Transmutation*, Mol, Belgium, 1998, published by OECD.
21 C. Erlinger, D. Gazeau, T. Zemb, C. Madic, L. Lefrançois, M. Hébrant and C. Tondre, *Solvent Extr. Ion Exch.*, 1998, **16**, 707.
22 D. M. Doddrell, D. T. Pegg and M. R. Bendall, *J. Magn. Reson.*, 1982, **48**, 323.
23 A. A. Maudsley and R. R. Ernst, *Chem. Phys. Lett.*, 1977, **50**, 368.
24 A. Bax, *Two-dimensional Nuclear Magnetic Resonance in Liquids*, Reidel, Dordrecht, 1982.
25 J. Jeener, B. H. Meier, P. Bachmann and R. R. Ernst, *J. Chem. Phys.*, 1979, **71**, 4546.
26 C. L. Perrin and T. M. Dwyer, *Chem. Rev.*, 1990, **90**, 935.
27 A. G. Redfield and S. Kunz, *J. Magn. Reson.*, 1975, **19**, 250.
28 D. Marion and K. Wüthrich, *Biochem. Biophys. Res. Commun.*, 1983, **113**, 967.
29 P. W. Anderson, *J. Phys. Soc. Jpn.*, 1954, **9**, 316.
30 R. Kubo, *J. Phys. Soc. Jpn.*, 1958, **9**, 935.
31 R. A. Sack, *Mol. Phys.*, 1958, **1**, 163.
32 M. L. Martin, J.-J. Delpuech and E. J. Martin, *Practical NMR Spectroscopy*, Heyden-Wiley, London, 1980, p. 442.
33 L. A. Laplanche and M. T. Rogers, *J. Am. Chem. Soc.*, 1963, **85**, 3728.
34 P. Laszlo, *Prog. Nucl. Magn. Reson. Spectrosc.*, 1967, **3**, 231.
35 C. C. Hinckley, *J. Am. Chem. Soc.*, 1969, **91**, 5160.
36 J. V. Hatton and R. E. Richards, *Mol. Phys.*, 1962, **5**, 139.
37 L. L. Graham, *Org. Magn. Reson.*, 1980, **14**, 40.
38 L. L. Graham, *J. Chem. Soc.*, *Perkin Trans. 2*, 1981, 1481.
39 M. Oki, *Applications of Dynamic NMR Spectroscopy to Organic Chemistry*, VCH, Deerfield Beach, FL, 1985, pp. 223 and 278.
40 J.-J. Delpuech, in *Dynamics of Solutions and Fluid Mixtures by NMR*, ed. J.-J. Delpuech, Wiley, Chichester, 1995, p. 90.
41 L. W. Reeves, R. C. Shaddick and K. N. Show, *Can. J. Chem.*, 1971, **75**, 3372.
42 G. Isaksson and J. Sandström, *Acta Chem. Scand.*, 1967, **21**, 1605.

Paper 9/00766K